THE JOURNAL OF PHYSICAL CHEMISTRY C
A JOURNAL OF THE AMERICAN CHEMICAL SOCIETY

pubs.acs.org/JPCC

Article

Liquid Pumping by Nanoscopic "Flexible Oars"

Lela Vuković and Petr Král*

Cite This: J. Phys. Chem. C 2021, 125, 8349−8352

Read Online

ACCESS | Metrics & More | Article Recommendations

ABSTRACT: Molecular dynamics simulations are used to study pumping of liquids by flapping graphene nanosheets. Despite the low Reynolds number conditions, liquids are pumped by the flapping nanosheets with an irreversible dynamics. Evaluation of the pumping rates as a function of frequency and amplitude of the flapping motion revealed that a "flexible oar" pumping mechanism can act at the nanoscale, where molecular systems behave as a coarse-grained macroscopic systems. These observations could be implemented in designing of motile nanoscale machines.

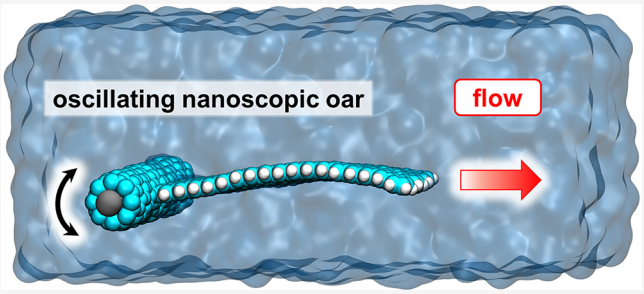

INTRODUCTION

Living organisms exploit various mechanisms to gain motility at different scales.[1] For example, bacteria can efficiently swim through liquids by rotating their flagella (5−20 μm long, 10−30 nm wide filaments)[2] or by beating with their cilia (3−10 μm long, <1 μm wide filaments).[3] Bacteria can swim at low Reynolds numbers, where a Brownian dynamics operates, by oscillating their microscopic filaments.[4] In this "flexible oar" mechanism, filaments periodically generate deformations propagating along their length and pulling the liquid.[4,5] Analogous pumping mechanisms could be used in synthetic systems.[6−15] For example, a flexible oar formed by a steel wire (d = 0.6 mm diameter, l = 30 cm length) can pump silicone oil at low Reynolds numbers of $Re = 10^{-2} - 10^{-3}$.[16]

All of the above systems operate with a continuous fluid, despite the presence of low Reynolds numbers. Here, we examine whether the flexible oar mechanism can be transferred all the way down to the molecular scale, where the assumption of a continuous fluid is breaking down. We use atomistic molecular dynamics (MD) simulations to model an oscillating flexible nanosheet and analyze its ability to pump liquids.

METHODS

Figure 1 shows a model graphene sheet covalently bonded to a carbon nanotube (CNT), which performs oscillatory rotation around its axis, but is otherwise restrained. Length and diameter of the selected model CNT are 2.82 and 0.62 nm, respectively. The studied paddles, containing 290−660 atoms, are l = 1.5−7.5 nm long, $w \approx$ 1.4 nm wide, and immersed in water boxes 62 × 49 × 245 Å^3 in volume. The CNT oscillatory rotation is obtained by applying an oscillatory force of $F_y = a_0 \sin(\omega t)$ in the y-direction (Figure 1, top) to CNT atoms which are connected to the graphene sheet. Since the CNT is freely rotating around a shaft, the force can rotate it in a range of $(-\pi/2,\pi/2)$ rad and induce the flapping motion of the graphene paddle.

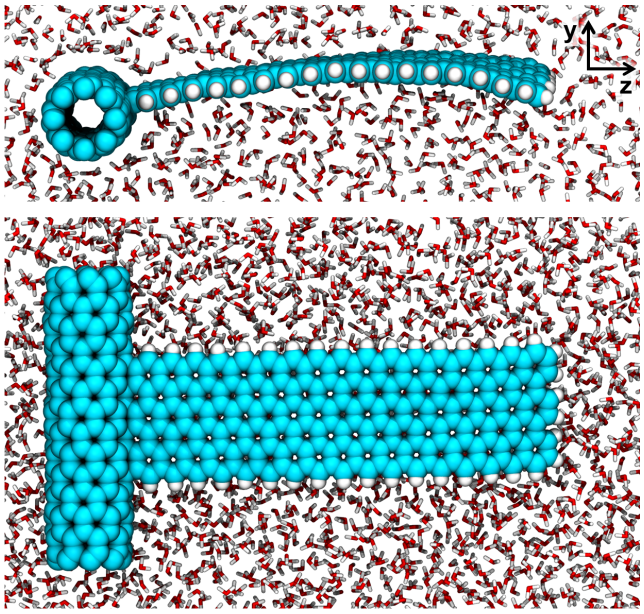

Figure 1. Side and top views of the flexible oscillating graphene sheet paddle in water. The edges of the graphene sheet are capped by hydrogen atoms.

Received: March 3, 2021
Revised: March 28, 2021
Published: April 7, 2021

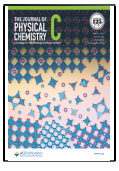

https://doi.org/10.1021/acs.jpcc.1c01906
J. Phys. Chem. C 2021, 125, 8349−8352

Here, the water pumping induced by the graphene sheet oscillation is studied by classical nonequilibrium atomistic MD simulations with the NAMD package[17] and the CHARMM force field.[18] Water is described with TIP3P model, and carbon atoms of CNT and graphene are described as typical aromatic carbon atoms within the CHARMM force field. The systems are simulated in NPT ensembles (p = 1 bar at T = 300 K) with periodic boundary conditions applied. The Langevin dynamics is used with a small damping coefficient of 0.01 ps^{-1}, in order to avoid unphysical dissipation of the linear and angular momenta;[19] the simulation time step is 2 fs. The water flow is calculated by averaging the number of solvent molecule crossing events at two xy-plane cross sections within the unit cell, where the upper and lower cross sections are defined at z = 1 and −2 nm within the unit cell.

RESULTS AND DISCUSSION

It might seem obvious that the oscillating nanopaddle from Figure 1 can pump liquids. However, according to the scallop theorem, pumping of liquids at low Reynolds numbers is only possible by paddles performing a time-irreversible motion,[4] as in the flexible oar mechanism, while oscillating rigid paddles cannot pump liquids. The necessity of some motional irreversibility emerges from the analysis of the fluid dynamics at low Reynold numbers. The Reynolds number describes the nature of fluid flow around constrictions (ratio of inertial and viscous forces), $Re = av\rho/\eta$, where a is a linear dimension of the system, v is a fluid velocity around it, ρ is a fluid density, and η is a dynamic viscosity of the fluid. For a graphene paddle in Figure 1, with parameters of $a = 10^{-8}$ m, v = 1 m/s, $\rho = 10^3$ kg/m^3, and $\eta = 10^{-3}$ Pa s, we obtain $Re \approx 10^{-2}$, while for a macroscopic paddle $Re \approx 10^6$. In low-Re environments, inertia is negligible (waves do not exist), so viscosity dominates the motion of objects. Therefore, pumping of liquids by paddles at low Re is only possible if we introduce some irreversibility in their dynamics, such as in a corkscrew motion performed by flagella.

Figures 2a,b shows selected simulation snapshots of $y(t)$ profiles of selected paddle atoms as a function of their distance z_C from CNT. These snapshots are obtained during one oscillation cycle of the paddle with parameters of l = 4.1 nm, $w \approx$ 1.4 nm, and A = 8.4 nN, and frequencies of (a) ω = 0.045 ps^{-1} and (b) ω = 0.15 ps^{-1}. At smaller oscillation frequencies (Figure 2a) the paddle seems to bend less. In contrast, at higher frequencies (Figure 2b) a deformation is clearly seen propagating along the paddle. We can expect that these more pronounced and denser deformations should pump more liquid.

In Figure 2c, we examine in more detail the time-dependent dynamics of a paddle (l = 6 nm) oscillating with a frequency of ω = 0.045 ps^{-1}. The blade motion is perfectly periodic at the CNT surface, but it becomes random with the growing separation from CNT. Moreover, we can see a phase shift mounting with the distance from CNT, which reveals that deformations are propagating along the paddle. However, the more random motion of the paddle seen further away from CNT contributes less to liquid pumping, so that pumping should level out for long paddles.

These results illustrate that the flapping nanoscopic paddle performs an irreversible motion, where periodic deformations unidirectionally propagate along its length. This pocket-like transport of liquids resembles motion of droplets on surfaces of CNTs oscillating in air.[20] However, these propagating

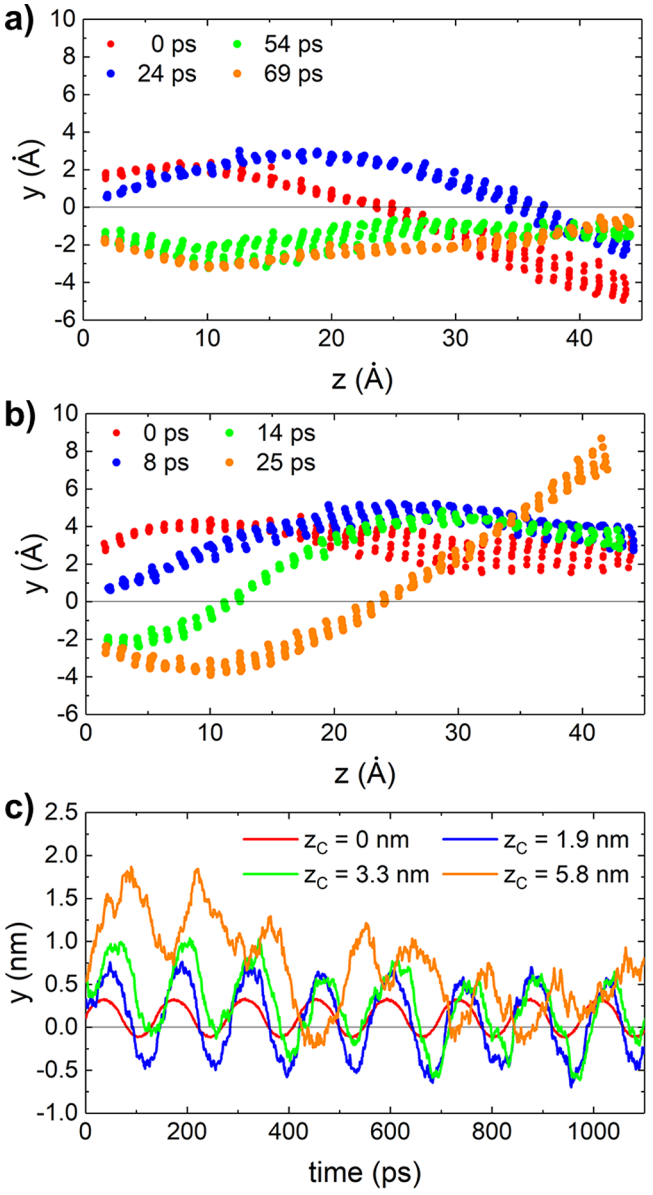

Figure 2. Snapshots of paddle shapes within a single oscillatory cycle for (a) ω = 0.045 and (b) 0.15 ps^{-1}. The force, $F_y = a_0 \sin(\omega t)$, with a_0 = 8.4 nN, is applied to atoms at $x \approx 0$ Å. The paddle has a length of l = 4.1 nm and a width of $w \approx$ 1.4 nm. (c) A time-dependent dynamics $y(t)$ of several selected paddle atoms (l = 6.0 nm), separated at z_C distance from the driven atoms on CNT. For this system, ω = 0.045 ps^{-1} and a_0 = 8.4 nN. With the increasing distance, the motion becomes more random.

deformations are not waves, since the paddle vibration is overdamped at low Re. The traveling deformations are determined by mechanical properties of the paddle, the fluid properties (damping), and the driving forces. The pumping rates should depend on the paddle length, width, its chemical functionalization, the frequency and amplitude of its driving.[6] Changes in CNT dimensions are likely to have only a small direct influence on the pumping rate, as long as the oscillatory force with suitable amplitude and frequency can be applied to CNT and thus also to one edge of the nanoscale paddle to induce its flapping motion.

Figure 3a shows the calculated flows of water and pentane separately driven by graphene paddles of different lengths and

https://doi.org/10.1021/acs.jpcc.1c01906
J. Phys. Chem. C 2021, 125, 8349−8352

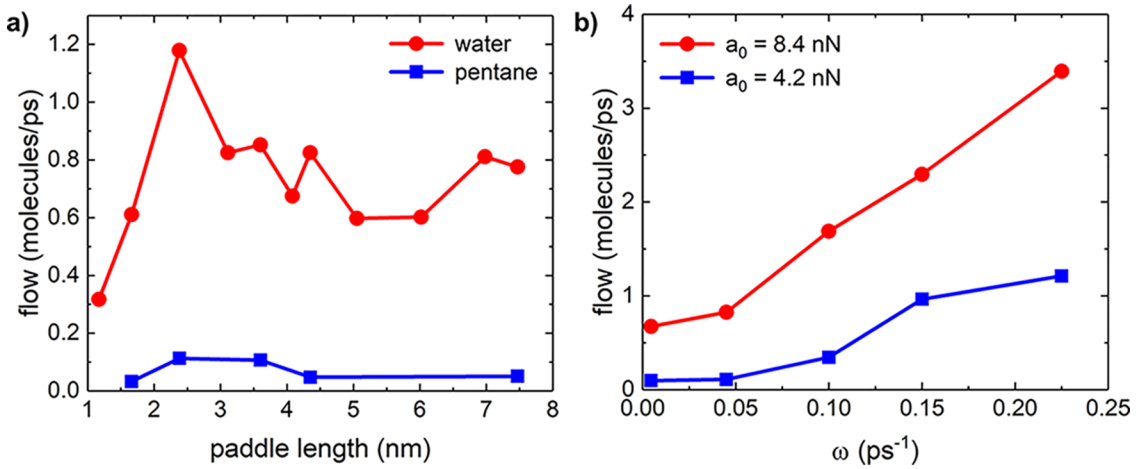

Figure 3. (a) Flows of water and pentane separately pumped by paddles of the length l when driven by an oscillating force, $F_y = a_0 \sin(\omega t)$, where a_0 = 8.4 nN is the amplitude and ω = 0.045 ps^{-1} is the oscillation frequency. (b) Flows of water pumped by the paddle of a l = 4.1 nm length, calculated for different a_0 as a function of ω.

a fixed width ($w \approx 1.4$ nm), oscillated at ω = 0.045 ps^{-1}. The slippery nature of the graphene paddle allows higher water flows, in analogy to carbon nanotubes.[21]

For paddles with very short lengths of $l \approx 1$ nm, the flow is very small since the paddle deformations are very small (reversibility − scallop theorem). For longer paddles, the flow increases and reaches a local maximum at $l_{opt} \approx 2-3$ nm where the paddles are irreversibly waving without much restriction. When the paddle lengths are further increased to $l > 3$ nm, the flow slightly drops and remains approximately constant. The long paddles cannot move freely because their long tails prevent them from oscillating even close to the source. Moreover, coherent oscillations do not propagate in distant regions of the paddles, as visualized from the random profiles (loss of coherence) of the paddle regions that are at large distances from the oscillation source (Figure 2c). Therefore, increasing the length of paddles has no effect on their pumping rates. The dependence of the water flow on the paddle length, shown in Figure 3a, resembles the length-dependence of a propulsive force generated by a macroscopic flexible tail oscillating in a viscous medium.[5,16] This underlines the fact that classicality is largely preserved at the nanoscale, despite the presence of fluid molecules comparable in size to the paddle.

Moreover, while the flow induced by the paddle in the same conditions is approximately 1 order of magnitude smaller for pentane than for water, the trends remain the same. We can identify two main reasons for this reduced pumping of pentane. The first reason is the wettability of the paddle; in general, molecules that stick to the paddle tend to clog it.[6] For graphene paddles, this happens for hydrophobic molecules like pentane. On the other hand, hydrophilic molecules can easily slip away from the paddle. The second reason is the length of the solvent molecules; longer pentane molecules can get interlocked and tend to be more intertwined than smaller water molecules.[6] Both reasons contribute to the fact that water can slip more easily from the paddle and thus get mixed and pumped, while pentane sticks to the paddles, gets interlocked, and significantly avoids the pumping.

Finally, Figure 3b shows the flow of water pumped by paddles (l = 4.1 nm) driven by forces of different amplitudes and frequencies. At both amplitudes, the water flow grows with the driving frequency, since the irreversibility becomes larger. The flow is growing in a nonlinear fashion with the driving amplitude. In the limit of low frequency, the flow would go to zero (in the present study, the frequencies examined are still relatively large). The pumping rates in Figure 3 were determined in simulations that neglect the polarizability of CNT, graphene paddle and water. Previous studies showed that water flow in polar boron-nitride nanotubes is smaller than in nonpolar CNTs, due to stronger interactions between water and polar nanotube walls resulting in increased friction.[22] Analogously, polarizability effects are expected to result in stronger interactions between water and the nanopaddle and the reduced pumping rate.

CONCLUSION

In summary, using MD simulations, we have shown that liquids can be pumped by molecular blades by the flexible oar mechanism, which is active at low Reynolds numbers. The pumping rates grow with the driving frequency, but they undergo a typical flattening in long nanopaddles. Moreover, the pumping becomes inefficient in liquids with large molecules comparable in size to the paddle length. Nevertheless, the obtained data support the idea that such nanoscale pumping of liquids should be possible to approximately describe by macroscopic equations valid at low Reynolds numbers, and here the molecular nature of pumped liquids can be seen as a coarse-graining of the continuous macroscopic models. In applications, the nanopaddle oscillations could be powered by piezoelectric means[23−25] and magnetic fields[26−28] and used to drive microscopic devices submerged in liquids.

AUTHOR INFORMATION

Corresponding Author

Petr Král − *Departments of Chemistry, Physics, Pharmaceutical Sciences, and Chemical Engineering, University of Illinois at Chicago, Chicago, Illinois 60607, United States;* orcid.org/0000-0003-2992-9027; Email: pkral@uic.edu

Author

Lela Vuković − *Department of Chemistry and Biochemistry, University of Texas at El Paso, El Paso, Texas 79968, United States;* orcid.org/0000-0002-9053-5708

https://doi.org/10.1021/acs.jpcc.1c01906
J. Phys. Chem. C 2021, 125, 8349−8352

Complete contact information is available at:
https://pubs.acs.org/10.1021/acs.jpcc.1c01906

Notes

The authors declare no competing financial interest.

■ ACKNOWLEDGMENTS

The authors would like to thank R. D. Astumian for helpful discussions.

■ REFERENCES

(1) Yadav, V.; Duan, W.; Butler, P. J.; Sen, A. Anatomy of nanoscale propulsion. *Annu. Rev. Biophys.* **2015**, *44*, 77−100.
(2) Brennen, C.; Winet, H. Fluid Mechanics of Propulsion by Cilia and Flagella. *Annu. Rev. Fluid Mech.* **1977**, *9*, 339−398.
(3) Gueron, S.; Liron, N. Ciliary Motion Modeling, and Dynamic Multicilia Interactions. *Biophys. J.* **1992**, *63*, 1045−1058.
(4) Purcell, E. M. Life at Low Reynolds Numbers. *Am. J. Phys.* **1977**, *45*, 3−11.
(5) Wiggins, C. H.; Riveline, D.; Ott, A.; Goldstein, R. E. Trapping and Wiggling: Elastohydrodynamics of Driven Microfilaments. *Biophys. J.* **1998**, *74*, 1043−1060.
(6) Wang, B.; Král, P. Chemically Tunable Nanoscale Propellers of Liquids. *Phys. Rev. Lett.* **2007**, *98*, 266102.
(7) Kim, Y. W.; Netz, R. R. Pumping Fluids with Periodically Beating Grafted Elastic Filaments. *Phys. Rev. Lett.* **2006**, *96*, 158101.
(8) Dreyfus, R.; Baudry, J.; Roper, M. L.; Fermigier, M.; Stone, H. A.; Bibette, J. Microscopic Artificial Swimmers. *Nature* **2005**, *437*, 862−865.
(9) Vuković, L.; Král, P. Coulombically Driven Rolling of Nanorods on Water. *Phys. Rev. Lett.* **2009**, *103*, 246103.
(10) Rapaport, D. C. Microscale Swimming: The Molecular Dynamics Approach. *Phys. Rev. Lett.* **2007**, *99*, 238101.
(11) Král, P.; Wang, B. Material Drag Phenomena in Nanotube. *Chem. Rev.* **2013**, *113*, 3372−3390.
(12) Li, J.; Rozen, I.; Wang, J. Rocket Science at the Nanoscale. *ACS Nano* **2016**, *10*, 5619.
(13) Qiu, T.; Lee, T.-C.; Mark, A. G.; Morozov, K. I.; Münster, R.; Mierka, O.; Turek, S.; Leshansky, A. M.; Fischer, P. Swimming by Reciprocal Motion at Low Reynolds Number. *Nat. Commun.* **2014**, *5*, 5119.
(14) Magdanz, V.; Khalil, I. S. M.; Simmchen, J.; Furtado, G. P.; Mohanty, S.; Gebauer, J.; Xu, H.; Klingner, A.; Aziz, A.; Medina-Sanchez, M.; Schmidt, O. G.; Misra, S. IRONSperm: Sperm-Templated Soft Magnetic Microrobots. *Sci. Adv.* **2020**, *6*, eaba5855.
(15) Huang, H.-W.; Uslu, F. E.; Katsamba, P.; Lauga, E.; Sakar, M. S.; Nelson, B. J. Adaptive Locomotion of Artificial Microswimmers. *Sci. Adv.* **2019**, *5*, eaau1532.
(16) Yu, T. S.; Lauga, E.; Hosoi, A. E. Experimental Investigations of Elastic Tail Propulsion at Low Reynolds Number. *Phys. Fluids* **2006**, *18*, 091701.
(17) Phillips, J. C.; et al. Scalable Molecular Dynamics with NAMD. *J. Comput. Chem.* **2005**, *26*, 1781−1802.
(18) MacKerell, A. D.; et al. All-Atom Empirical Potential for Molecular Modeling and Dynamics Studies of Proteins. *J. Phys. Chem. B* **1998**, *102*, 3586−3616.
(19) Servantie, J.; Gaspard, P. Methods of Calculation of a Friction Coefficient: Application to Nanotubes. *Phys. Rev. Lett.* **2003**, *91*, 185503.
(20) Russell, J.; Wang, B.; Král, P. Nanodroplet Transport on Vibrated Nanotubes. *J. Phys. Chem. Lett.* **2012**, *3*, 353−357.
(21) Zhao, Y.; Chen, J.; Huang, D.; Su, J. The Role of Interface Ions in the Control of Water Transport through a Carbon Nanotube. *Langmuir* **2019**, *35*, 13442−13451.
(22) Vuković, L.; Vokac, E.; Král, P. Molecular Friction-Induced Electroosmotic Phenomena in Thin Neutral Nanotubes. *J. Phys. Chem. Lett.* **2014**, *5*, 2131−2137.
(23) Král, P.; Mele, E. J.; Tománek, D. Photogalvanic Effects in Heteropolar Nanotubes. *Phys. Rev. Lett.* **2000**, *85*, 1512.
(24) Mele, E. J.; Král, P. Electric Polarization of Heteropolar Nanotubes as Geometric Phase. *Phys. Rev. Lett.* **2002**, *88*, 056803.
(25) Wang, Z. L.; Song, J. Piezoelectric Nanogenerators based on Zinc Oxide Nanowire Arrays. *Science* **2006**, *312*, 242−246.
(26) Tierno, T.; Golestanian, R.; Pagonabarraga, I.; Sagues, F. Controlled Swimming in Confined Fluids of Magnetically Actuated Colloidal Rotors. *Phys. Rev. Lett.* **2008**, *101*, 218304.
(27) Snezhko, A.; Belkin, M.; Aranson, I. S.; Kwok, W.-K. Self-Assembled Magnetic Surface Swimmers. *Phys. Rev. Lett.* **2009**, *102*, 118103.
(28) Li, J.; Sattayasamitsathit, S.; Dong, R.; Gao, W.; Tam, R.; Feng, X.; Ai, S.; Wang, J. Template Electrosynthesis of Tailored-made Helical Nanoswimmers. *Nanoscale* **2014**, *6*, 9415−9420.